Low-Loss MEMS Band-Pass Filters with Improved Out-of-Band Rejection by Exploiting Inductive Parasitics

Yonghyun Shim[1], Roozbeh Tabrizian[2], Farrokh Ayazi[2], and Mina Rais-Zadeh[1]

[1]Department of Electrical Engineering & Computer Science, University of Michigan, Ann Arbor, MI 48109, USA
[2]School of Electrical & Computer Engineering, Georgia Institute of Technology, Atlanta, GA 30308, USA

Abstract

This paper reports on a new implementation of integrated lumped filters with improved out-of-band rejection and pass-band loss. Inductive parasitics are exploited to provide additional transmission zeros at the high frequency end, which can improve both the out-of-band rejection and roll-off. Thick silver is electroplated to reduce the insertion loss and achieve high quality factor. An insertion loss of better than 3dB has been achieved for filters across 220MHz to 640MHz with unloaded *Q* as high as 50. The out-of-band rejection of filters is as high as 60dB. These are believed to be the highest performing integrated filters in terms of out-of-band attenuation and spurious-free response implemented on silicon substrate.

Introduction

MEMS-based resonators and filters will find increasing applications in communication systems. In recent years much effort has been focused on increasing the quality factor (*Q*) and improving the insertion loss of MEMS filters [1], [2]. With the rapid adoption of new wireless technologies, the frequency spectrum is becoming increasingly crowded, escalating the demand for high-performance integrated filters with high out-of-band rejection and spurious-free response. To effectively suppress strong interferer signals, an attenuation of more than 50dB is recommended for filters in RF front-end receiver [3]. On the other hand, tunability is a feature that is equally attractive as the fabrication errors are indispensible and post fabrication trimmings are costly. For tunable filters, high level of attenuation combined with a spurious- and harmonic-free response has not been reported in the literature as non-linear components are generally used to achieve tuning. This paper presents the first implementation of high-performance passive tunable filters with high out-of-band rejection that are suitable for multi-standard communication systems. Fabricated filters are in the frequency range of 220MHz to 640MHz and show insertion loss of better than 3dB and out-of-band rejection as high as 60dB on silicon substrate. A single-input multiple-output filter array is also demonstrated by arraying three such filters connected to the same node with a passive matching network.

Bandpass Filter Design

The Common practice to improve the out-of-band rejection of bandpass filters includes increasing the order of the filter [4] and cascading a number of filters [5] at the cost of increased size and pass-band loss. In this work, a high out-of-band rejection is achieved through the use of inductive parasitics that are inherent to any MEMS tunable capacitor. Filters are designed in coupled-resonator configurations, which is desirable for filters having bandpass *Q*s of 10 or more [6]. Tuning of coupled-resonator filters is also simpler since all nodes are resonated to the same frequency.

The general form of a capacitively-coupled-resonator configuration is shown in Fig. 1. To achieve tuning, dual-gap MEMS lateral tunable capacitors are incorporated in the filter, as discussed in [7]. The electrical model and response of the incorporated tunable capacitors are presented in Figs. 2 and 3. The tunable capacitors are modeled as a sense capacitor (C_{1t}) in series with a parasitic inductor representing the spring (L_{1p}) and a parasitic capacitor representing the actuator (C_{1p}).

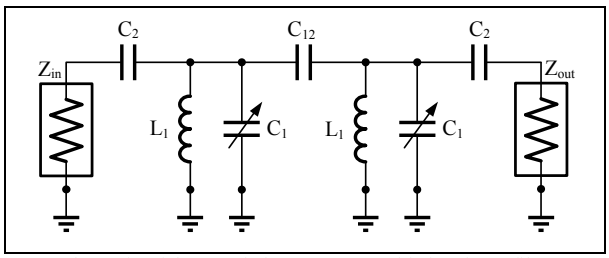

Figure 1. Schematic of the coupled-resonator tunable bandpass filter.

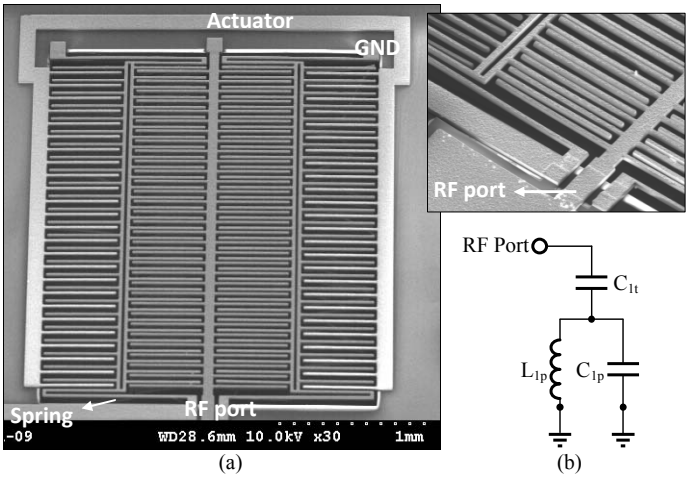

Figure 2. (a) SEM view of the tunable capacitor, and (b) the electrical model of the tunable capacitor. The inset shows a close-up SEM view of the interdigitated fingers. The actuation gap is 20μm and the sense gap is 10μm.

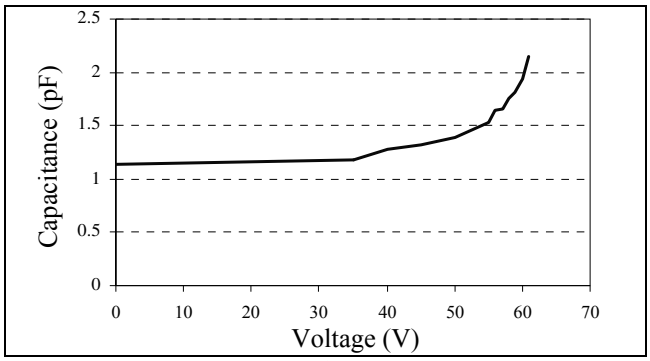

Figure 3. (a) Measured tuning and (b) embedded characteristic of the tunable silver capacitor. The trade-line of the measured data is shown for the quality factor.

Fig. 4 shows the final electrical model of the filter, considering the parasitics. When designing the filters, values of the tunable capacitor (C_{1t} in Fig. 4), fixed capacitor (C_{1f}), matching capacitor (C_2) and inductor (L_1) are selected with the following considerations while maintaining a narrow 3-dB BW for the filters: 1) the matched impedance of the filter is 50Ω. 2) The 50-dB rejection bandwidth is < 700MHz. 3) the insertion loss is < 3dB, and 4) a tuning range is > 100MHz. To achieve the aforementioned requirement, a transmission zero is placed at the high frequency end of the filter. The frequency of the transmission zero is controlled by the value of C_{1t}, C_{1f}, C_{1p} and L_{1p} (the parasitic inductance of the springs). To realize the required capacitance at each node, a fixed capacitor (C_{1f}) is placed in parallel with the tunable capacitor (C_{1t}).

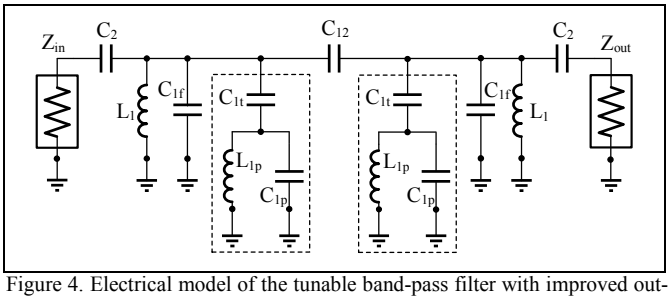

Figure 4. Electrical model of the tunable band-pass filter with improved out-of-band rejection.

Using these guidelines several filters have been designed in the 220MHz−640MHz frequency range. Electrical design simulations of the filters are first performed in Agilent ADS. The optimizations of the physical design (layout) of the filter and the individual lumped components are performed in Ansoft HFSS 3D modeler. The thickness of the electroplated silver, the routing layer, and the silicon dioxide interlayer dielectric is assumed to be 30μm, 4μm, and 2μm, respectively. The loss tangent of silicon dioxide at 640MHz is assumed to be 0.002. Figs. 5 and 6 show the simulated response of two filters centered at 480MHz and 640MHz, each having a 3-dB bandwidth of ~40MHz and insertion loss < 3dB. As shown, the out-of-band rejection of filters is better than 50dB.

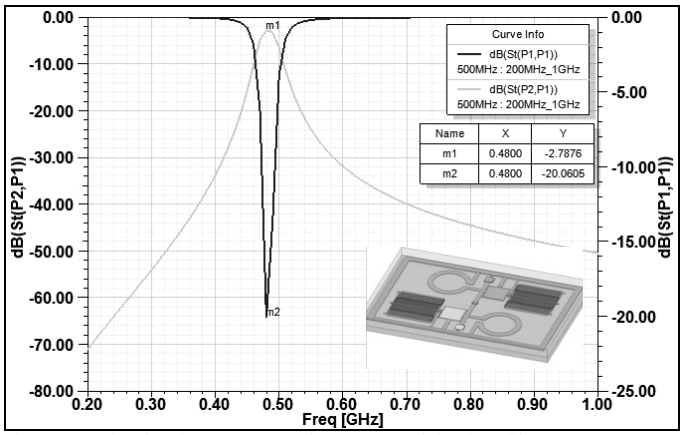

Figure 5. Simulated response and HFSS model of a filter at 480MHz, showing an IL of 2.79dB and out-of-band rejection of better than 50dB.

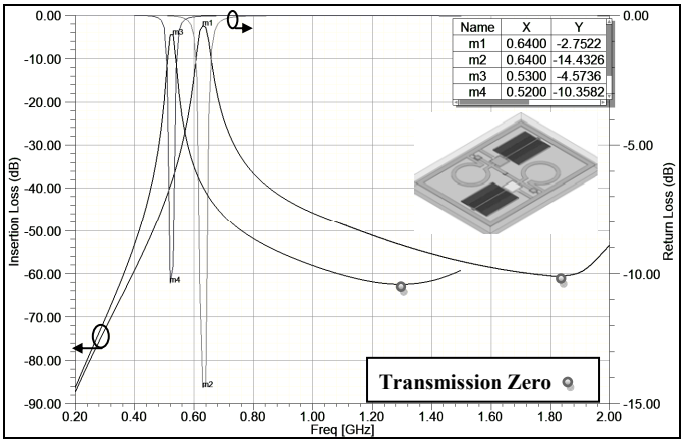

Figure 6. Simulated response and HFSS model of a filter at 640MHz at the initial state and the maximum tuned state (520MHz). The IL increases from 2.7dB to 4.6dB when the filter is tuned. The out-of band rejection is ~60dB. The frequency of the transmission zero decreases as the filter is tuned.

Measurement Results

Filters are implemented using the fabrication technique outlined in [7]. On-wafer S-parameter measurements of the fabricated devices have been carried out using an Agilent 8364B PNA and SOLT calibration. The pad parasitics were not de-embedded.

A. Individual Filter Results

The measured out-of-band rejection of filters is better than 50dB as shown in Figs. 7 and 8. In addition, filters exhibit a very high unloaded Q of >44, the highest reported for UHF tunable filters on silicon. The unloaded Q is extracted from the measured frequency response using the following expression: $Q_u = \frac{f_0/BW}{1-S_{21}(f_0)}$. The tuning characteristic of an exemplary MEMS filter at 640MHz is shown in Fig. 9. Continuous tuning is achieved by applying DC voltages to the isolated actuator port of the tunable capacitors. Tuning can be significantly improved by increasing the thickness of the electroplated silver- thereby increasing the tunable to fixed capacitance ratio.

For comparison, the same filter is also implemented using off-chip inductors from coilcraft [8] (Fig. 10(a), (b)). The air-core off-chip inductor has a Q of 120 at 640MHz while the Q of on-chip inductor is ~90. The filter with higher-Q off-chip inductors exhibits lower performance due to the loss of interconnects, illustrating the benefits of integration to achieve low insertion loss (compare Figs. 8 and 10(c)).

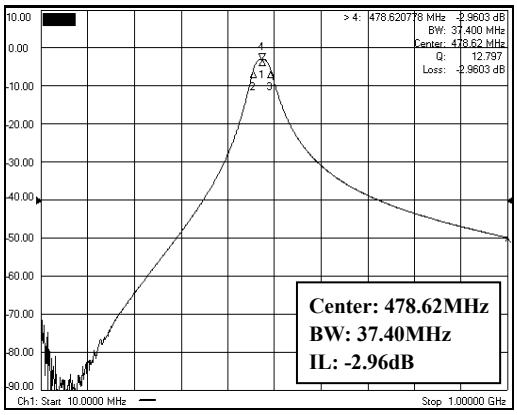

Figure 7. Measured response of the filter at 480MHz. The transmission zero is at 1.5GHz (not captured in this image). The unloaded Q of the filter is 44.

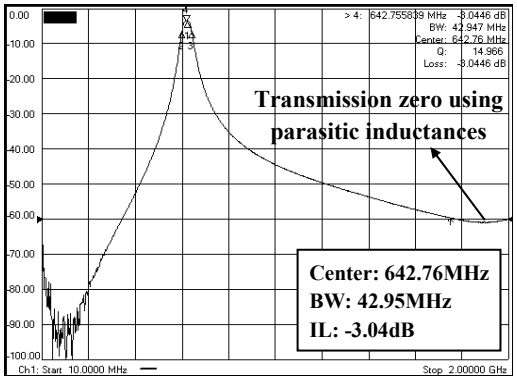

Figure 8. Measured response of the silver filter at 640MHz, showing an out-of-band rejection of > 60dB. The unloaded Q of the filter is 50, the highest reported for integrated MEMS filters on silicon.

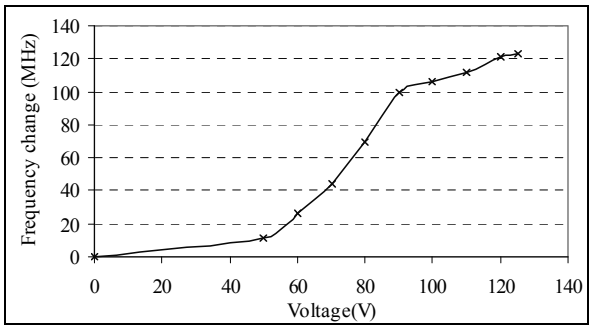

Figure 9. Measured tuning characteristic of a silver filter (coated with Parylene-C for improved tuning). Tuning is achieved by applying DC voltages to isolated actuation ports of the tunable capacitors shown in Fig. 2. The tuning range can be improved by increasing the aspect ratio of the capacitor gap (aspect ratio is 3 in this case).

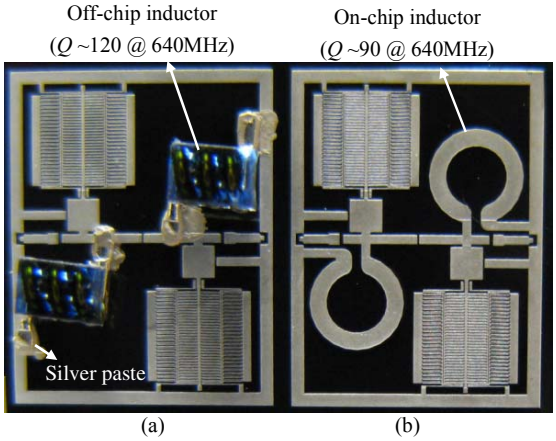

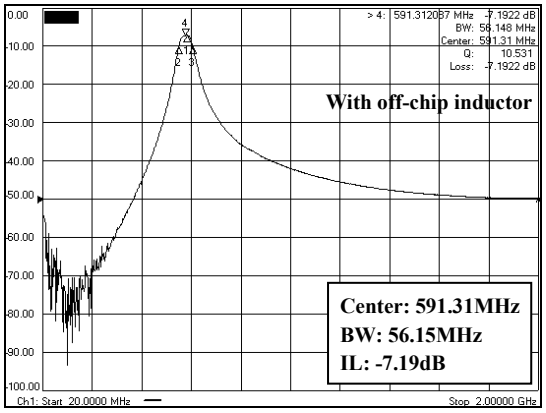

(c)

Figure 10. Micrographs of the 640MHz filter (a) using off-chip inductors and (b) fully integrated on silicon. (c) Measured response of the filter at 640MHz using off-chip inductors from coil-craft, showing significantly lower performance compared to the integrated counterpart (compare to Fig. 8). This is due to the capacitive and resistive parasitics of the silver paste and the pads used to connect the off-chip inductor on the silicon die.

B. Array Implementation Results

Three filters with high out-of-band rejection are connected to the same input port to realize, for the first time, a three-way filter array fully integrated on silicon. The array can be used

to receive and transmit signals in three different bands, simultaneously. Fig. 11 shows the configuration and a SEM picture of the three-way filter with outputs centered at 208MHz, 470MHz, and 630MHz. A passive matching network is designed at the input port as shown in Fig. 11. The matching network provides 50Ω matching between the input port of the filter array and each bandpass filter and minimizes the reflection at the input of the filters. The simulated and measured response of three-way array is shown in Figs. 12 and 13, respectively. When placed in the array, the insertion loss of filters slightly increases and the bandwidth decreases due to the loss of the matching network and the minor interaction of the filters. The highest frequency filter suffers from the largest drop in the insertion loss since the parasitics of the long routing lines become more pronounced at higher frequencies. The performance of the filter array can be further improved by increasing the Q of matching components and reducing the length of interconnects. The matching network can be made tunable to provide proper matching across the entire tuning range of the filters.

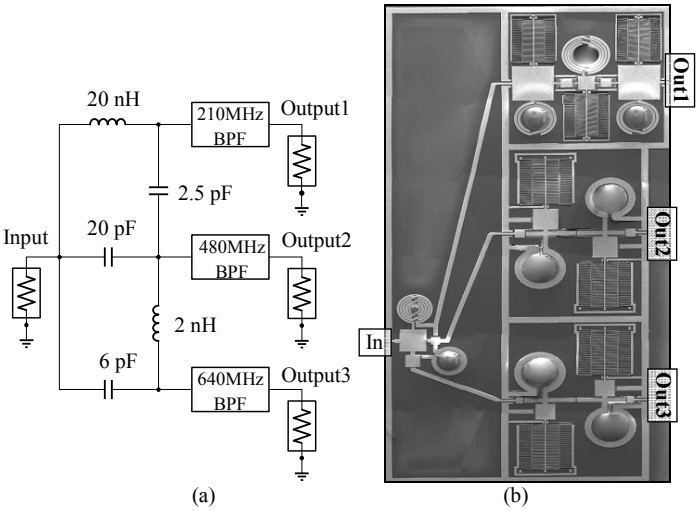

Figure 11. (a) Configuration, and (b) SEM image of the three-way filter array.

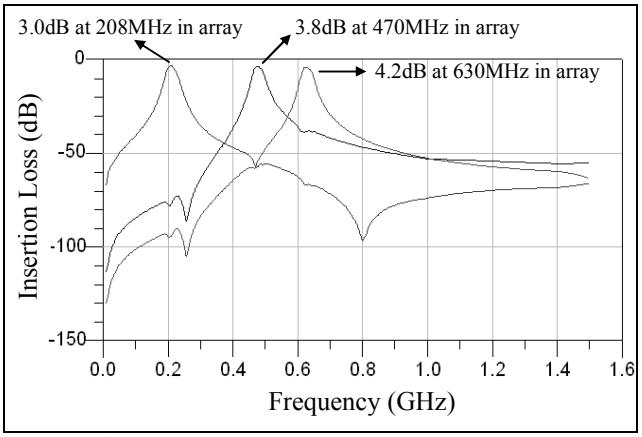

Figure 12. Simulated response of the three-way filter array showing small interaction between them due to the high stop-band rejection of the filters.

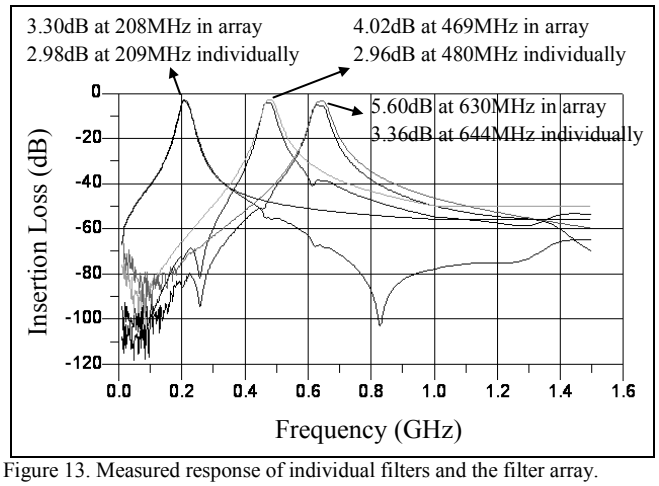

Figure 13. Measured response of individual filters and the filter array.

Conclusions

Design and characterization of several high-performance integrated silver bandpass filters were presented. An insertion loss of better than 3dB, and bandwidth smaller than 45MHz have been achieved for filters across 220MHz to 640MHz. High out-of-band rejection (> 50dB) is achieved through the use of inductive parasitics. A three-way filter array is implemented taking advantage of small interaction between the filters due to the high out-of-band rejection. The measured data are in good agreement with the simulations.

Acknowledgement

This project was funded by DARPA under the Analog Spectral Processors (ASP) program. Authors would like to thank the staff at the Michigan Nanofabrication Facilities (LNF) and Georgia Tech Microelectronic Research Center (MiRC) for their assistance.

References

[1] R. M. Young et al., "Low-loss bandpass RF filter using MEMS capacitance switches to achieve a one-octave tuning range and independently variable bandwidth," *IEEE MTT-S International Microwave Symposium*, vol. 3, pp. 1781-1784, June 2003.

[2] K. Entesari, K. Obeidat, A. R. Brown, and G. M. Rebeiz, "A 25-75-MHz RF MEMS Tunable Filter," *IEEE Transaction on Microwave Theory and Technique*, vol. 55, no. 11, pp. 2399-2405, Nov. 2007.

[3] M. A. Dubois et al., "Monolithic above-IC resonator technology for integrated architectures in mobile and wireless communication," *IEEE Journal of Solid-State Circuits*, vol. 41, no. 1, pp. 7-16, Jan. 2006.

[4] M. R. Lababidi et al., "High resistive silicon based low-pass active filter design for TV on mobile application," *IEEE MTT-S International Microwave Symposium,* pp. 1053-1056, June 2009.

[5] M. Rais-Zadeh, A. Kapoor, H. M. Lavasani, and F. Ayazi, "Fully integrated low-loss bandpass filter for wireless applications," *Journal of Micromachining and Microengineering*, vol. 9, July 2009.

[6] A. B. Williams and F. J. Taylor, "Electronic filter design handbook," *McGraw Hill, Inc*, second edition, 1988.

[7] M. Rais-Zadeh and F. Ayazi, "Small-bandwidth integrated tunable bandpass filters for GSM applications," *IEEE Int. Conference on Microelectromechanical Systems (MEMS'08),* pp.1032-1035, Jan. 2008.

[8] Coilcraft Air Core Inductors, http://www.coilcraft.com/pdfs/micro.pdf.